Supplementary Information for

Historical transboundary ozone health impact linked to affluence

Lulu Chen, Jintai Lin, Ruijing Ni, Hao Kong, Mingxi Du, Yingying Yan, Mengyao Liu, Jingxu Wang, Hongjian Weng, Yuanhong Zhao, Chunjin Li, Randall V. Martin

***Correspondence to: Jintai Lin (linjt@pku.edu.cn)**

This document includes:

Supplementary Tables:

Supplementary Figures:

Supplementary Tables

Supplementary Table 1: Population-weighted annual average MDA8 ozone over different regions.

	Model ozone before bias adjustment (ppbv)	Model ozone after bias adjustment (ppbv)	Observation (ppbv)	Relative model bias after adjustment
Mainland China	49.9	41.0	39.2	4.6%
US	43.6	35.7	33.4	6.3%
Europe	35.4	30.1	34.4	-14.1%
Canada	37.9	31.6	33.7	-6.0%
World	46.6	37.9	37.6	0.8%

Supplementary Table 2: Geographical information of 13 background sites for ozone measurement from TOAR[1]. All data are downloaded from https://join.fz-juelich.de/access/.

Station name	Country	Latitude/Longitude	Altitude (m)	Dates
Lisboa/Gago Coutinho	Portugal	38.77°N/9.13°W	105.0	1971-2002
Sibton	United Kingdom	52.29°N/1.46°E	46.0	1973-2012
Stevenage	United Kingdom	51.89°N/0.20°W	90.0	1976-1994
Zugspitze	Germany	47.42°N/10.98°E	2960.0	1978-2010
Harwell	United Kingdom	51.571°N/1.33°W	126.0	1976-2012
Hohenperssenberg	Germany	47.80°N/11.01°E	985.0	1971-2017
Barrow	United States of America	71.323°N/156.61°W	11.0	1973-2018
Mauna Loa	United States of America	19.53°N/155.58°W	3397.0	1973-2018
American Samoa GMD Observatory	American Samoa	14.25°S/170.56°W	42.0	1976-2015
Amundsen-Scott South Pole	Antarctica	89.99°S/24.8°E	2841.0	1975-2018
Jeløya	Norway	59.43°N/10.6°E	5.0	1979-2003
Whiteface Mountain Summit, New York	United States of America	44.37°N/73.90°E	1483.0	1975-2015

Supplementary Figures

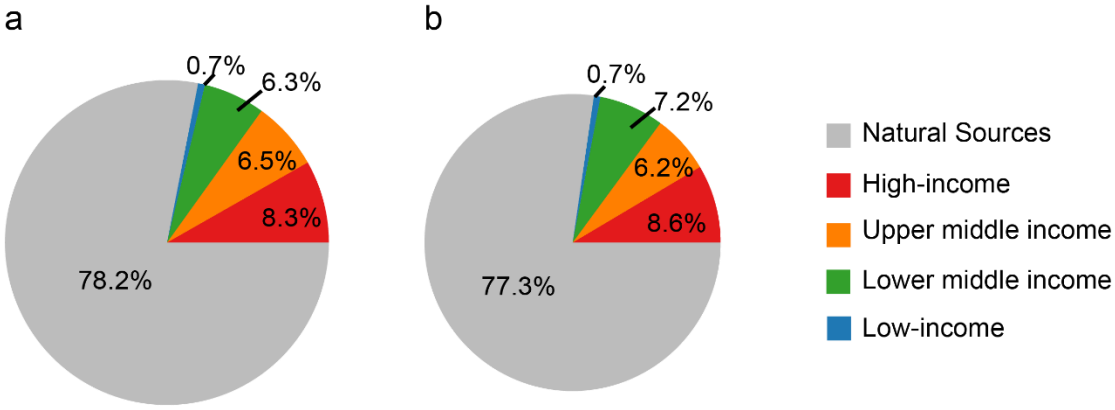

Supplementary Figure 1: Global premature mortality attributable to ozone exposure in 1981, as well as contributions by individual source regions. (a) the calculation based on GEOS-Chem simulations driven by meteorological conditions in 2014. (b) similar to (a) but using meteorological conditions in 1981. The ozone exposure-response model is from Turner et al.[2], with the LCC at 26.7 ppbv.

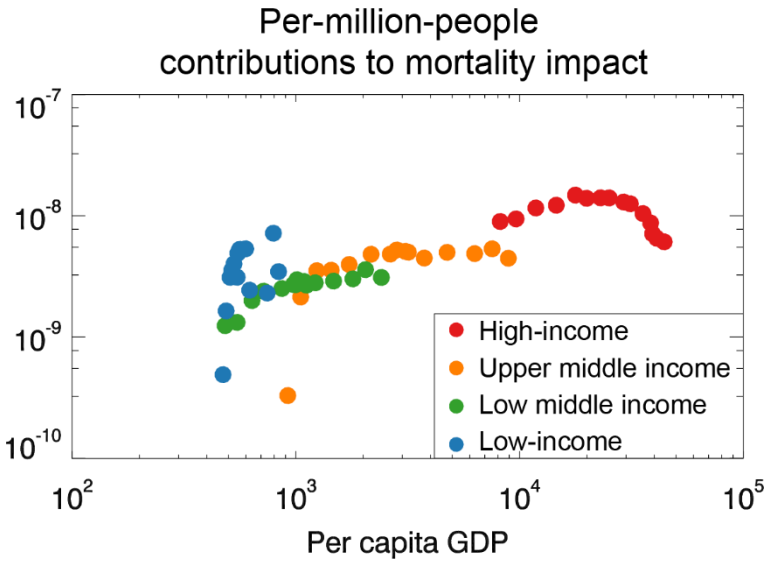

Supplementary Figure 2: Relationship between regional affluence level and its mortality impact caused by transboundary ozone. Similar to Fig. 4a, but using LCC = 0 ppbv.

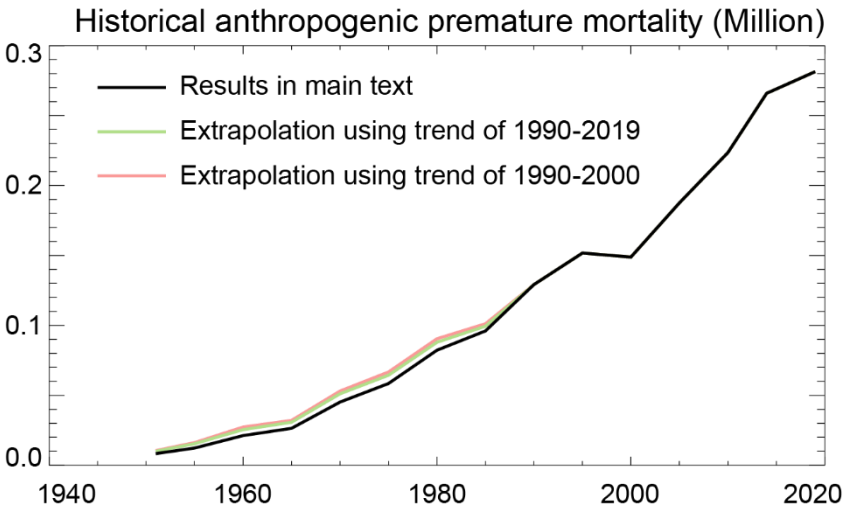

58

59 **Supplementary Figure 3: Historical changes in anthropogenic ozone related**
60 **premature deaths.** The baseline mortality rates before 1990 are fixed at the year of
61 1990 (black line), extrapolated based on the corresponding trends over 1990-2014
62 (green line) and over 1990-2000 (pink line), respectively.

63

64

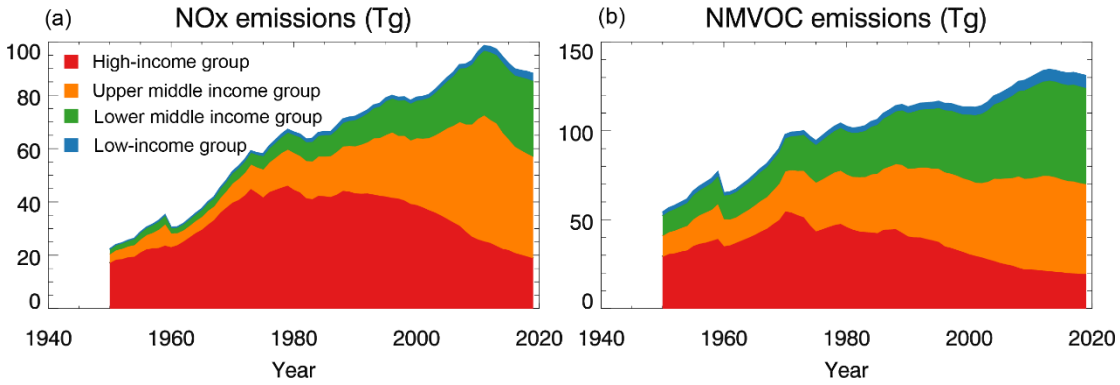

Supplementary Figure 4: Historical changes in anthropogenic emissions of NO_x and NMVOC. The emission data are taken from CEDS[3, 4] and MEIC[5-7].

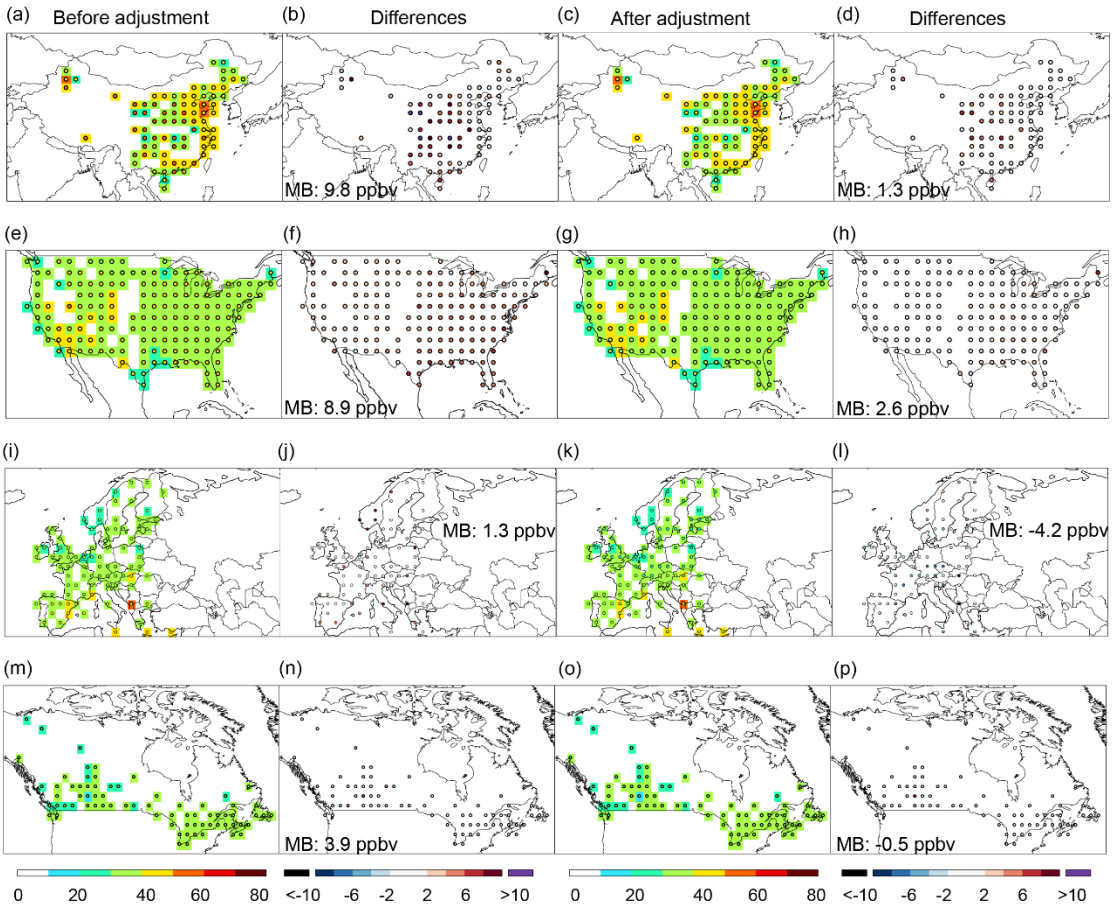

Supplementary Figure 5: Evaluation of annual average MDA8 ozone. The panels show simulated (colored circles) and observed (colored squares) ozone and their differences over mainland China, the United States, Europe and Canada in 2014. The number in each panel shows the mean bias (MB).

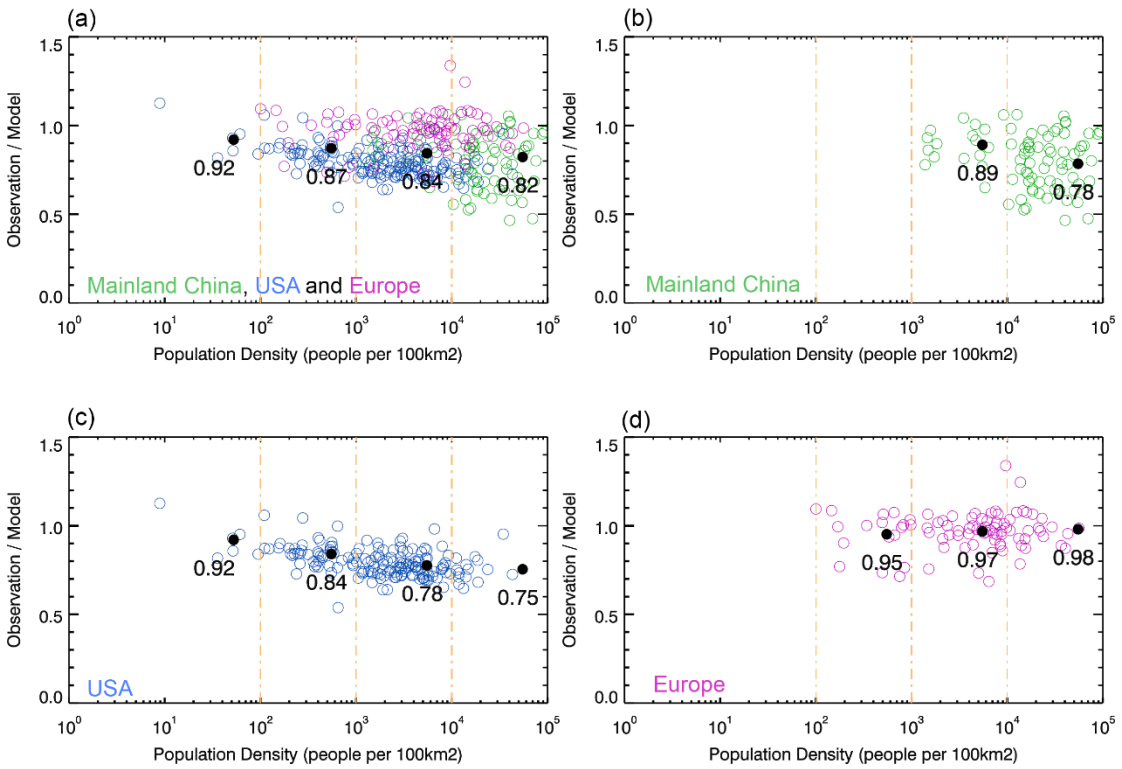

75

76 **Supplementary Figure 6: Ratio of observed to modeled annual mean MDA8 ozone**
77 **over mainland China, the United States and Europe.** Each circle denotes a grid cell
78 with available observations. Each black dot denotes the average of all circles in each
79 population density bin separated by the yellow vertical line.

80

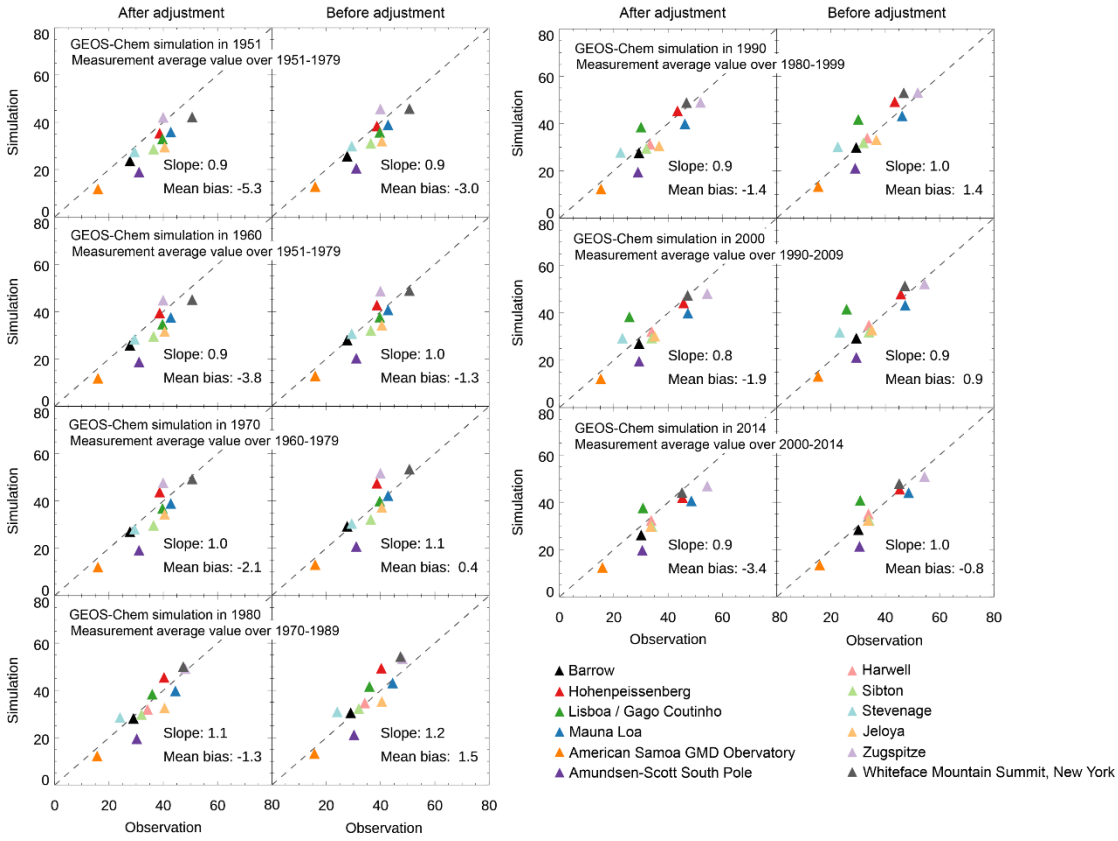

Supplementary Figure 7: Evaluation of modeled historical ozone concentrations. Each scatter plot compares the observed and modeled decadal MDA8 ozone concentrations at individual background sites.

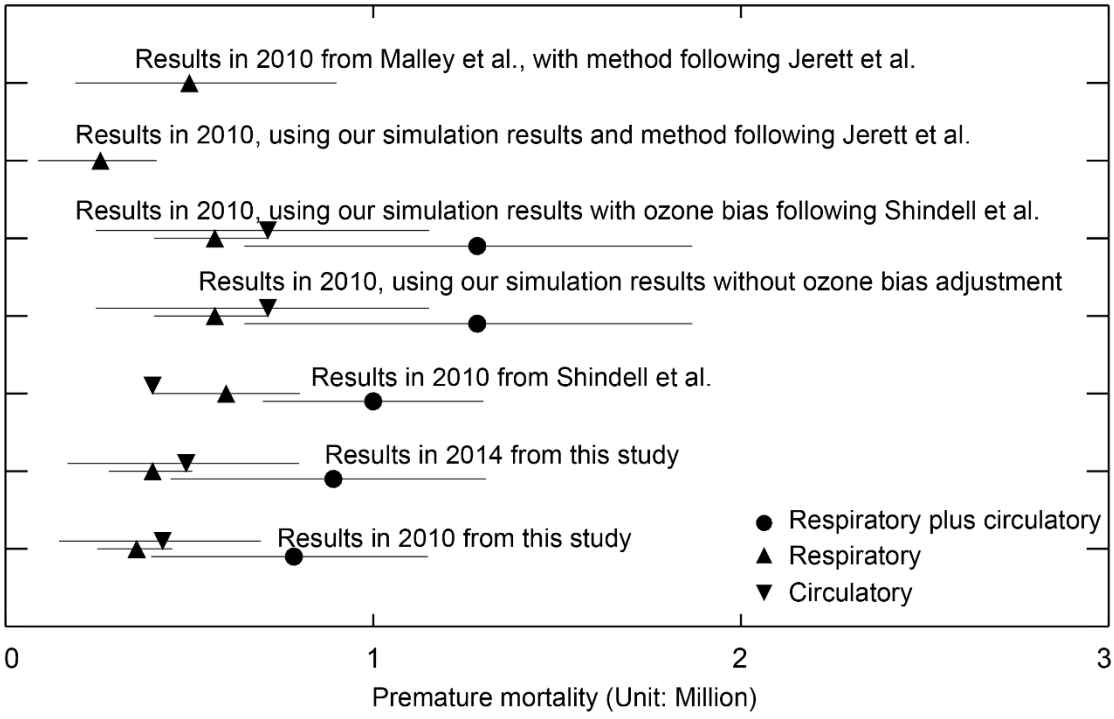

Supplementary Figure 8: Comparison between our results and previous studies. The mortality here is caused by both anthropogenic and natural ozone. Our results in 2010 and 2014 are consistent with the results in 2010 from Shindell et al.[8]. The results without bias adjustment and with bias adjustment following Shindell et al. [8] are all consistent with Shindell et al.[8]. Our estimate using Jerrett et al.[9] instead of Turner et al.[2] for exposure-response calculation (as another sensitivity test) is comparable to Malley et al.[10], both without ozone bias adjustment.

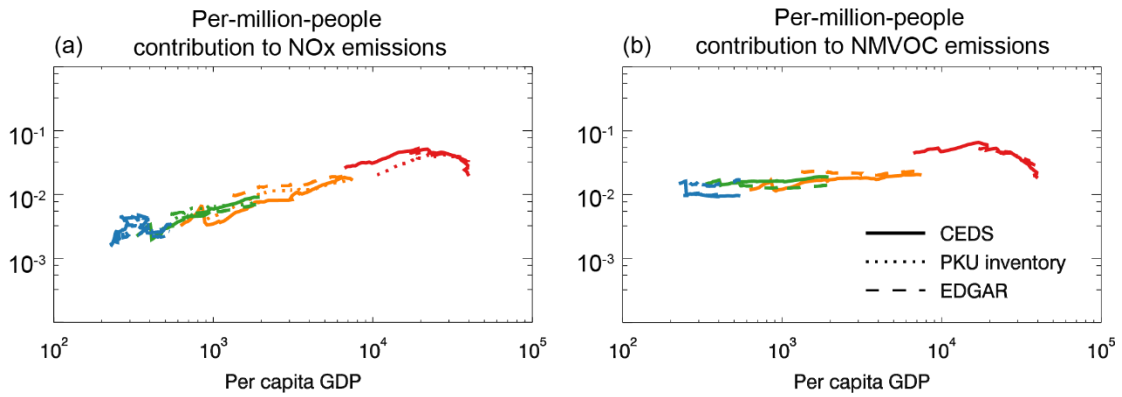

Supplementary Figure 9: Linking regional affluence level to its per-million-people contribution to its ozone precursors' emissions. The y-axis shows the per-million-people contribution to NOx (a) and NMVOC (b) emissions of four groups. The anthropogenic emission datasets include CEDS[3]+MEIC[5-7, 11] (solid lines), EDGAR v50[12] (dash lines) and PKU inventory[13-17] (dot lines). The x-axis shows per capita GDP of each source region.

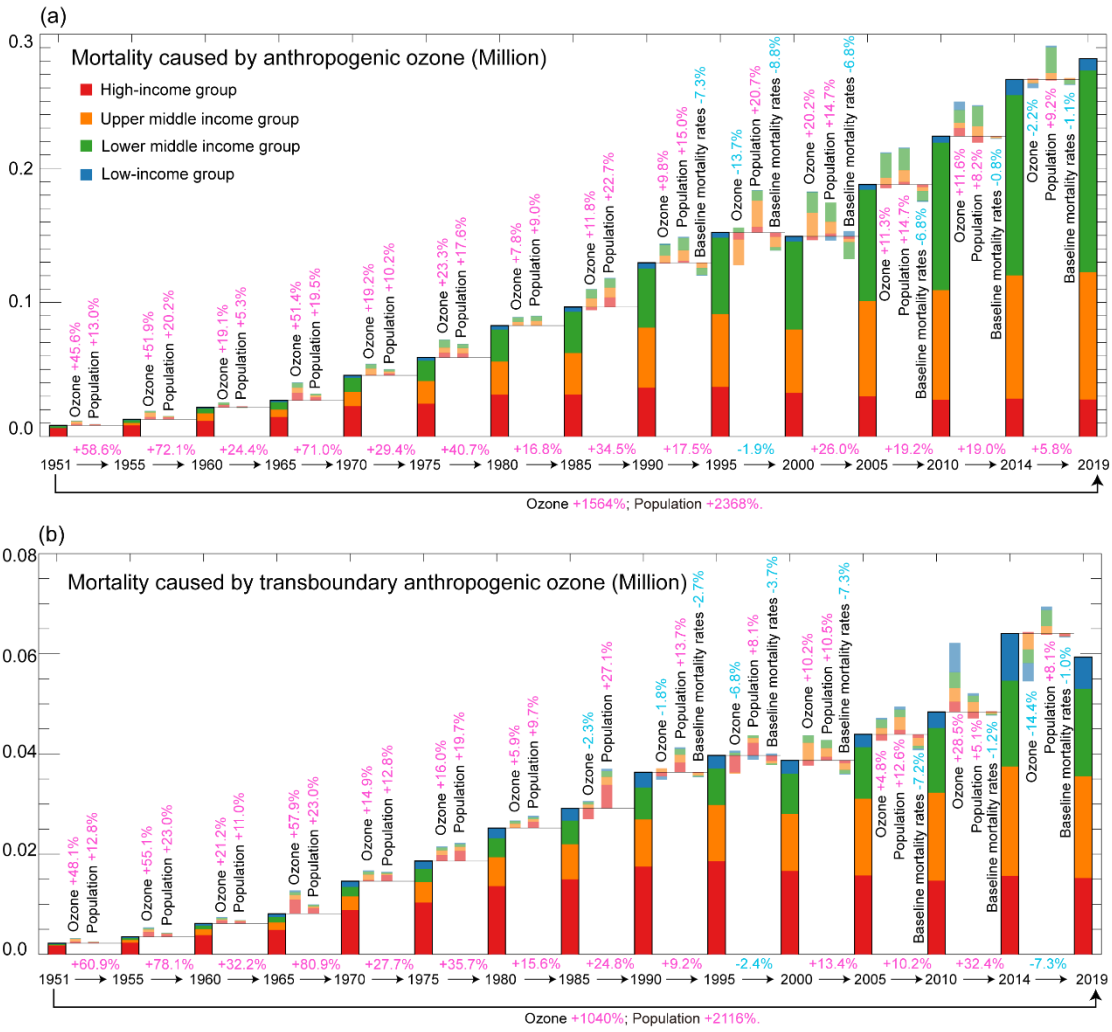

Supplementary Figure 10: Historical anthropogenic ozone related mortality and contributions from three driving factors. Similar to Figure 1 but for all simulation years. The y-axis shows the premature deaths attributable to total ozone (a) and transboundary ozone (b) caused by anthropogenic emissions in four income groups. The changes in baseline mortality rates before 1990 is not considered here, due to limitation in data availability.

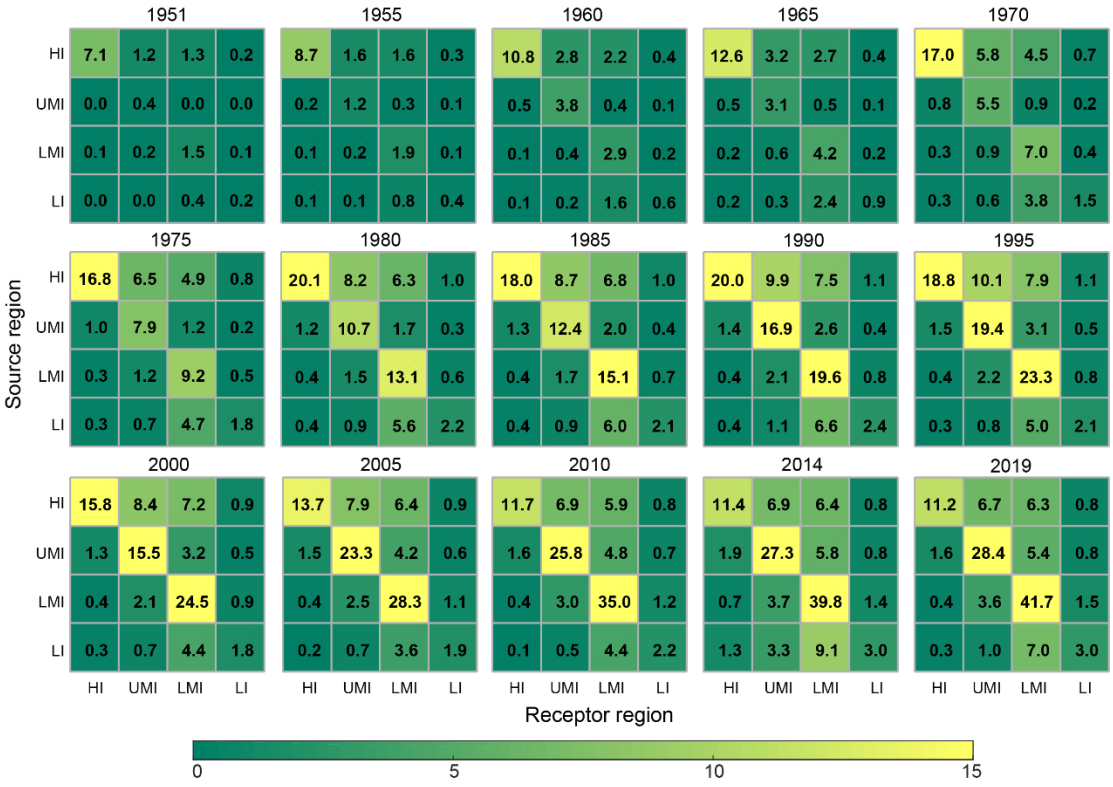

111

112 **Supplementary Figure 11: Bi-directional transboundary ozone related health**
113 **responsibility.** Similar to Figure 3 but for all simulation years. Each cell in the grid
114 shows the premature deaths in a receptor region due to anthropogenic emissions per
115 million people in a source region.

116

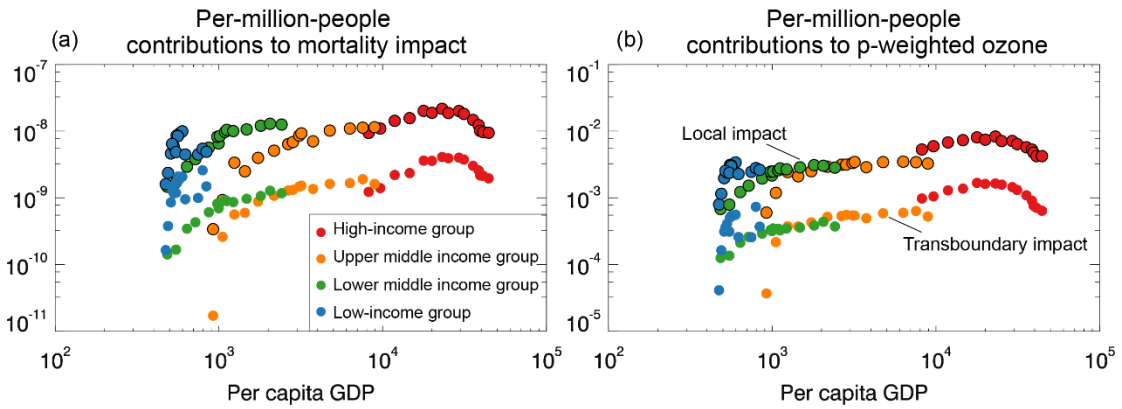

117

118 **Supplementary Figure 12: Relationship between regional affluence level and its**
119 **ozone impact.** The y-axis shows the ratio of deaths to total population (a) and
120 population-weighted MDA8 ozone (b) within its territory (circles with black coats) and
121 outside its territory (circles without coats) caused by per million residents in each source
122 region.

123

References

[1]. Tropospheric Ozone Assessment Report (TOAR) — Elementa Forums and Special Features.

[2]. Turner MC, Jerrett M, Pope CA, 3rd, Krewski D, Gapstur SM, Diver WR, et al. 2016 Long-Term Ozone Exposure and Mortality in a Large Prospective Study. *Am J Respir Crit Care Med*.193(10) 1134-42.

[3]. Hoesly RM, Smith SJ, Feng LY, Klimont Z, Janssens-Maenhout G, Pitkanen T, et al. 2018 Historical (1750-2014) anthropogenic emissions of reactive gases and aerosols from the Community Emissions Data System (CEDS). *Geoscientific Model Development*.11(1) 369-408.

[4]. McDuffie EE, Smith SJ, O'Rourke P, Tibrewal K, Venkataraman C, Marais EA, et al. 2020 A global anthropogenic emission inventory of atmospheric pollutants from sector- and fuel-specific sources (1970-2017): an application of the Community Emissions Data System (CEDS). *Earth System Science Data*.12(4) 3413-42.

[5]. Zheng B, Tong D, Li M, Liu F, Hong C, Geng G, et al. 2018 Trends in China's anthropogenic emissions since 2010 as the consequence of clean air actions. *Atmospheric Chemistry and Physics*.18(19) 14095-111.

[6]. Li M, Liu H, Geng G, Hong C, Liu F, Song Y, et al. 2017 Anthropogenic emission inventories in China: a review. *National Science Review*.4(6) 834-66.

[7]. Multi-resolution Emission Inventory for China. Available at: http://www.meicmodel.org; last access: 18 Nov 2018.

[8]. Shindell D, Faluvegi G, Seltzer K, Shindell C. 2018 Quantified, localized health benefits of accelerated carbon dioxide emissions reductions. *Nat Clim Chang*.8(4) 291-5.

[9]. Jerrett M, Burnett RT, Pope CA, 3rd, Ito K, Thurston G, Krewski D, et al. 2009 Long-term ozone exposure and mortality. *N Engl J Med*.360(11) 1085-95.

[10]. Malley CS, Henze DK, Kuylenstierna JCI, Vallack HW, Davila Y, Anenberg SC, et al. 2017 Updated Global Estimates of Respiratory Mortality in Adults ⩾ 30Years of Age Attributable to Long-Term Ozone Exposure. *Environ Health Perspect*.125(8) 087021.

[11]. Geng GN, Zhang Q, Martin RV, Lin JT, Huo H, Zheng B, et al. 2017 Impact of spatial proxies on the representation of bottom-up emission inventories: A satellite-based analysis. *Atmospheric Chemistry and Physics*.17(6) 4131-45.

[12]. Crippa M, Solazzo E, Huang G, Guizzardi D, Koffi E, Muntean M, et al. 2020 High resolution temporal profiles in the Emissions Database for Global Atmospheric Research. *Sci Data*.7(1) 121.

[13]. Huang T, Zhu X, Zhong Q, Yun X, Meng W, Li B, et al. 2017 Spatial and temporal trends in global emissions of nitrogen oxides from 1960 to 2014. *Environ Sci Technol*.51(14) 7992-8000.

[14]. Huang Y, Shen H, Chen H, Wang R, Zhang Y, Su S, et al. 2014 Quantification of global primary emissions of $PM_{2.5}$, PM_{10}, and TSP from combustion and industrial process sources. *Environ Sci Technol*.48(23) 13834-43.

[15]. Wang R, Tao S, Shen H, Huang Y, Chen H, Balkanski Y, et al. 2014 Trend in global black carbon emissions from 1960 to 2007. *Environ Sci Technol*.48(12) 6780-7.

[16]. Meng W, Zhong Q, Yun X, Zhu X, Huang T, Shen H, et al. 2017 Improvement of a global high-resolution ammonia emission inventory for combustion and industrial sources with new data from the residential and transportation Sectors. *Environ Sci*

Technol.51(5) 2821-9.

[17]. Huang Y, Shen HZ, Chen YL, Zhong QR, Chen H, Wang R, et al. 2015 Global organic carbon emissions from primary sources from 1960 to 2009. *Atmos Environ*.122 505-12.